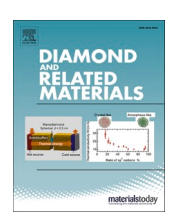
ELSEVIER

Contents lists available at ScienceDirect

# Diamond & Related Materials

journal homepage: www.elsevier.com/locate/diamond



# Dielectric performance of aluminum cation modified graphene oxide membrane: Influence of Al source

Yijing Y. Stehle a,\*, Maren Friday a, Timothy J. Barnum b, Qin Zou c

- <sup>a</sup> Department of Mechanical Engineering, Union College, Schenectady, NY 12308, USA
- <sup>b</sup> Chemistry Department, Union College, Schenectady, NY 12308, USA
- <sup>c</sup> Research Center for Nano Biomaterials, Analytical & Testing Center, Sichuan University, Chengdu 610064, China

### ARTICLE INFO

# Keywords: Graphene oxide (GO) Aluminum cation Dielectric constant Dielectric loss Capacitor

### ABSTRACT

This study demonstrates a facile and effective strategy for modifying the dielectric properties of graphene oxide membranes for applications in advanced energy storage devices. The high dielectric constant and low dielectric loss of graphene oxide (GO) make GO-based materials good dielectric separators for developing thin and flexible devices. Controllable tailoring of the dielectric properties of GO membranes is crucial to advance its applications as a dielectric material. Metal cation modification represents one tailoring strategy, but the effects of cation modification are difficult to compare due to its dependence on the metal cation source and the specific physicochemical conditions. In this study, we explore the dielectric properties of GO membranes modified by the introduction of  $Al^{3+}$  from different chemical sources. The dielectric constant and dielectric loss of an unmodified GO membrane and three  $Al^{3+}$  modified GO (AGO) membranes were measured in the frequency range from 1 Hz to  $10^6$  Hz, and the performance of a dielectric capacitor fabricated by sandwiching the GO (AGO) membrane between carbon paper electrodes was evaluated by cyclic voltammetry. Results demonstrate that the three different sources of  $Al^{3+}$  differently impact the dielectric properties of GO membranes and thus the performance of as-fabricated dielectric capacitors. Our results advance the fundamental understanding of how metal cation modification impacts the dielectric properties of GO membranes and demonstrate the possibility of designing membranes with controllable dielectric performance.

### 1. Introduction

Unlike graphene, which is a highly conductive semimetal 2D material, graphene oxide (GO), which is composed of monolayer graphene sheets decorated with abundant oxygenated functional groups (OFGs) on the edge (carboxyl groups) and plane (hydroxyl, carbonyl, and carboxyl groups), is nonconductive [1,2]. These oxygenated functional groups not only serve as structural defects that cut off the charge transfer route between the GO sheet resulting in a high dielectric constant with low dielectric loss, but also bond the adjacent GO sheets together when forming GO membranes [3–6]. During membrane formation, the OFGs serve as the joints connecting the adjacent GO sheets, which not only guide the lamination process, but also are responsible for the dissembling of the GO sheet in an aqueous environment during vibration or shearing [1]. The dielectric properties of GO are frequency dependent and sensitive to any structural changes of the OFGs. In addition, coordination with metal cations and polymer additives also impacts

dielectric performance [4,6]. The high dielectric constant (order of  $10^6$ ) and low dielectric loss of GO sheets [6-10] make it ideal for application as a dielectric material in capacitors, supercapacitors, and actuators [11,12].

It was widely reported that multivalent metal cation (e.g., Na<sup>+</sup>, Ca<sup>2+</sup>, Mg<sup>2+</sup>, Fe<sup>3+</sup>, or Al<sup>3+</sup>) coordination is very effective in improving the aqueous stability, ion selectivity, and mechanical strength of GO membranes [13–18]. Generally speaking, high valent metal cations show superior stability and strength improvements compared to bivalent and monovalent ones [15–18]. Multivalent metal cations can interact with GO sheets through stronger dative bonding with OFGs, electrostatic attraction to negatively charged functional groups, and cation– $\pi$  interactions with the sp²-conjugated structure of the graphene part of GO sheets. Multivalent metal cations are normally added into the GO in the form of either metal oxide, salt, or metal. The interaction between the metal cation and OFGs on the edge and basal plane of GO sheets is highly dependent on the chemical source used to introduce the metal cations

E-mail address: stehley@union.edu (Y.Y. Stehle).

<sup>\*</sup> Corresponding author.

### Γ19.201.

Robertson et al. modified graphene oxide sheets by introducing Al<sup>3+</sup> ions from either Al<sub>2</sub>O<sub>3</sub>, AlCl<sub>3</sub>, or Al foil into the acidic GO solution prior to membrane self-assembly [19]. It was experimentally observed that Al<sub>2</sub>O<sub>3</sub> does not significantly react with water to form Al<sup>3+</sup> ions. Therefore, remaining alumina particles disrupt the lamellar structure and decrease the GO membrane stability. Conversely, both AlCl3 and Al foil did significantly react with water to form Al<sup>3+</sup> ions, which increased crosslinking between GO sheets. Both AGO (Al foil) and AGO (AlCl<sub>3</sub>) membranes were more stable in water under mechanical stresses relative to unmodified GO, with the AGO (Al foil) membrane possessing the greatest aqueous stability. Introduction of Al<sup>3+</sup> from these different aluminum-containing precursors impacted the final structure and stability of AGO membranes. Since metal cations can bridge GO sheets through coordination to OFGs and the dielectric properties of GO are highly dependent on OFGs, it is anticipated that introduction of Al<sup>3+</sup> from different Al sources will similarly impact the dielectric properties of GO membranes in unique ways.

In this work, AGO membranes were prepared by dissolving alumina, aluminum chloride, and aluminum foil into acidic GO solution before forming laminated GO membranes under ambient conditions. This precoordination process allows metal cations to be coordinated with GO sheets in the solution and hold these sheets together during the lamination, or so-called self-assembly. The differing chemical preparation leads to different dielectric properties of the resulting AGO membranes. To better understand the influence of  $\mathrm{Al}^{3+}$  from different sources on the dielectric property of the GO membrane, the dielectric constant and dielectric loss of unmodified GO and three different AGO membranes were measured in the frequency range of 1 to  $\mathrm{10}^6$  Hz. In addition, the electrochemical performance of carbon paper capacitors with GO/AGO membrane dielectric layers was assessed by cyclic voltammetry experiments.

### 2. Experimental

Graphene oxide water dispersions were purchased from Graphenea (Cambridge, MA). Alumina powder (activated, neutral, Brockmann I), aluminum chloride hexahydrate (Sigma Aldrich, ReagentPlus, 99 %), Aluminum (Al) foil (0.024 cm thick, Puratronic, 99.997 % purity, Alfa Aesar) were used as Al3+ sources. The Al3+ ions were incorporated into the GO membranes by a simple pre-coordination process. Each Alcontaining species was added to the acidic GO solution in equal stoichiometric Al/GO ratio and membranes were subsequently formed via a self-assembly process at ambient conditions [19]. This method allows for controllable introduction of Al<sup>3+</sup> to the solution from sources that react differently in acidic solution before membrane formation. Experimental tests show that further increasing the amount of Al<sup>3+</sup> added can result in wrinkled surfaces for AGO (Al2O3) and surface cracks for AGO (AlCl<sub>3</sub>) and AGO (Al foil). Previous studies on the AGO (Al foil) showed that further increasing the amount of Al<sup>3+</sup> does not dramatically impact dielectric performance of AGO membranes [20]. A dynamic light scattering analyzer (Zetasizer Ultra, Malvern, Worcestershire, UK) was used to evaluate the surface charge of unmodified and modified GO solutions (4 mg/mL). Free-standing GO and AGO membranes were prepared under ambient evaporation drying process (21 °C, humidity of 40-50 %) in a Teflon evaporating dish [20]. GO and AGO membranes were sandwiched in between two 1 cm  $\times$  1 cm carbon paper electrodes as spacers in the dielectric capacitor. 0.6 cm wide copper foil tape was used as the current collector. The dielectric properties of GO and AGO membranes were studied by Electrochemistry Impedance spectra (EIS) in the frequencies ranging from 1 Hz to 1 MHz at room temperature with a CH 600E impedance analyzer [20]. The capacitive performance and long-term stability of GO and AGO membrane based dielectric capacitors in a potential of  $\pm 1$  V under different scan rates were analyzed by cyclic voltammetry.

### 3. Results and discussion

The frequency dependence of the dielectric constant (DiC) and dielectric loss (DiL) of GO and AGO membranes in the frequency range from 1 Hz to 1 MHz are shown in Fig. 1. The DiC and DiL of the fabricated capacitors are estimated based on impedance data (Fig. S1) using Eqs. (1), (2), and (3),

$$\varepsilon = \varepsilon' + i\varepsilon'' = \frac{d\cdot Z'}{A\cdot 2\pi f\cdot |Z|^2} - i\frac{d\cdot Z''}{A\cdot 2\pi f\cdot |Z|^2}$$
(1)

$$DiC = \varepsilon_r = \frac{\varepsilon'}{\varepsilon_0} = \frac{d \cdot Z'}{A \cdot 2\pi f \cdot |Z|^2 \cdot \varepsilon_0}$$
 (2)

$$DiL \approx \tan \delta = \frac{Z^{"}}{Z}$$
 (3)

where  $\varepsilon$  is the complex permittivity (F·m<sup>-1</sup>), Z is the complex impedance (Ohm), f is the frequency (Hz), A represents the metal foil area (m<sup>2</sup>), d is the separation between the plates in meters,  $\varepsilon_r$  is the relative permittivity or DiC, and  $\varepsilon_0$  is the vacuum electric permittivity ( $\varepsilon_0 \approx 8.854 \times 10^{-12} \ \text{F} \cdot \text{m}^{-1}$ ). Single primes indicate the real component of the permittivity or impedance and double primes indicate the imaginary component of each quantity. At the highest measured frequency (1 MHz), both unmodified and Al<sup>3+</sup> modified GO membranes show similar DiC value of  $5 \pm 0.5$  and the DiC increases with decreasing frequency for all GO based membranes, which is in good agreement with a previous study [20]. For unmodified GO membranes, the DiC approaches a maximum value of 240 at 1 Hz. Previous reports have demonstrated that compressed GO sheets, in which GO nanosheets are randomly packed and not bonded with each other, have a high DiC value of 10<sup>6</sup> at 1 Hz [6]. Vacuum-filtered GO membranes, in which GO nanosheets are partially bonded with each other during lamination, exhibit DiC values around 103 [4]. Relative to these materials, the self-assembled GO membranes in this study have lower DiC, but better integrity and stability [19]. The DiL of the GO membranes increase from 0.4 at 1 MHz to a maximum value of 0.9 at 0.1 MHz, then slowly decreases to minimum value of 0.25 at low frequency.

Among the three Al<sup>3+</sup> sources, Al<sub>2</sub>O<sub>3</sub> is most effective in increasing the DiC of GO, reaching 5500 at 1 Hz. The DiL increased to 1.0-1.2 in the frequency range below 0.1 MHz. The higher DiC value means AGO (Al<sub>2</sub>O<sub>3</sub>) membrane-based capacitors have the potential to exhibit better performance than pristine GO membrane-based capacitors, while the higher DiL value indicates greater energy dissipation. For AGO modified with Al3+ from AlCl3, the DiC increases rapidly below 10 kHz up to a value of 2600 at 1 Hz. AGO (AlCl<sub>3</sub>) has low dielectric loss (0.02) at high frequency and displays a clear peak (2.1) in the dielectric loss spectrum at 200 Hz. Therefore, AGO (AlCl<sub>3</sub>) has higher DiC and DiL values than pristine GO membrane for capacitors in the low frequency range (10 Hz  $\sim 1$  kHz). Among the three AGO, the AGO (Al foil) membrane is the only one that exhibits a lower DiC than unmodified GO membrane. AGO (Al foil) also has low dielectric loss (0.05) at high frequency, which increases to a maximum value higher than that of unmodified GO when f < 100 Hz. Even with the introduction of Al at identical stoichiometric Al/GO ratios, dielectric modification is highly dependent on the identity of the  $Al^{3+}$  precursor.

Energy dissipation in a dielectric material can occur mainly by conduction effects, which dominate at very low frequencies, and by polarization effects, which encompass several mechanisms over many orders of frequency. Interfacial polarization, related to the interplanar distance for through-plane GO measurements as in this study, dominates at low frequency (f < 10 Hz) for dielectrics [21]. The low-frequency dielectric loss values of all three types of AGO membranes are higher than that of pristine GO membranes due to the increase in the d-space after modification [20]. Dipolar polarization refers to the reorientation of molecular dipoles as the polarization of the electric field changes

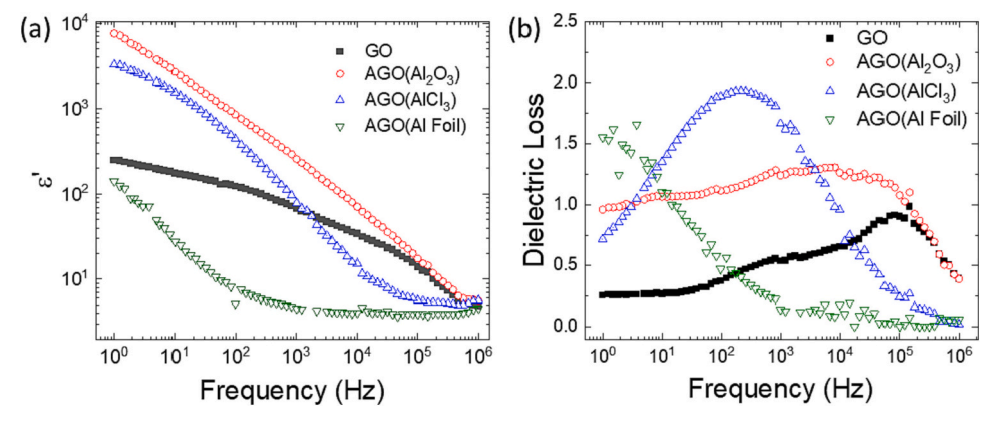


Fig. 1. Frequency dependence of dielectric constant (a) and dielectric loss (b) for GO and AGO membranes.

direction. The dielectric loss peaks around the resonance frequency of the dipole reorientation [21,22]; this frequency is related to the moment of inertia of the polar OFGs, and is strongly impacted by coordination with  $Al^{3+}$  ions. As observed from our previous physical-chemical property study, no obvious structure defects are formed during the  $Al^{3+}$  modification, and  $Al^{3+}$  interacts with the GO sheet through cation- $\pi$ , coordination, and electrostatic interactions. In this work, the DiL peak shifts to lower frequency following  $Al^{3+}$  modification in the order GO > AGO(Al $_2$ O $_3$ ) > AGO (AlCl $_3$ ) > AGO (Al foil). This order reflects an increase in  $Al^{3+}$  complexation with the OFGs on the GO sheet previously determined for  $Al^{3+}$  incorporation with these precursors [19]. As the moment of inertia of the polar OFGs decorated on the edge of the GO sheet increases, a lower resonance frequency for the dipolar polarization is observed.

Since the dielectric behavior of GO is highly dependent on the OFGs decorated on the GO sheet and their interactions, modification of OFGs on the GO nanosheet is an effective strategy for tuning the electric and dielectric properties of GO. To this end, we performed zeta potential measurements, shown in Fig. 2, of the GO and AGO aqueous dispersions prior to membrane self-assembly. Zeta potential relates to the density of negatively charged OFGs on the nanosheet surface, and previous work shows that oxidation level and pH value alter the zeta potential of GO nanosheets through chemical modification of the surface OFGs [23–25]. Introduction of Al<sup>3+</sup> cations to the GO dispersions can similarly alter zeta potential by electrostatic interaction between Al<sup>3+</sup> and the negatively charged surface OFGs. Fig. 2 shows that GO, AGO (AlCl<sub>3</sub>), and

AGO (Al<sub>2</sub>O<sub>3</sub>) dispersions show similar zeta potential values of -47 mV. Our previous work showed that the partial reduction of GO with the addition of Al<sup>3+</sup> from Al metal foil causes a decrease in the number of carboxylic acid and hydroxyl surface groups [19]. This is further supported by the change in zeta potential of AGO (Al foil) to -16 mV from -47 mV for the unmodified GO. This decrease in the magnitude of the zeta potential additionally supports the greater membrane stability of AGO (Al foil). In a previous study, we observed that aqueous solutions of GO, AGO (Al<sub>2</sub>O<sub>3</sub>), and AGO (AlCl<sub>3</sub>) form homogeneous solutions upon sonication, while AGO (Al foil) membranes decomposed into flakes made of large intact pieces of membrane [19]. The low zeta potential is consistent with this increased propensity for flocculation of AGO (Al foil). Unlike the Al<sup>3+</sup> modification with Al<sub>2</sub>O<sub>3</sub>, which does not obviously impact either pH value or oxidation level, the Al<sup>3+</sup> modification with AlCl<sub>3</sub> slightly decreases the pH value and increases the oxidation level of the GO solution [19]. However, no obvious zeta potential change was observed for the AGO (AlCl<sub>3</sub>) and AGO (Al<sub>2</sub>O<sub>3</sub>) solutions relative to the unmodified GO solution.

To explain the effect of Al<sup>3+</sup> modification from three different sources on the dielectric performance of GO membrane, Fig. 3 shows a schematic of the proposed microscopic structure of the GO membranes studied here. The graphene sheets of GO (gray line) are conductive and can serve as the electrodes, while OFGs (blue) are not conductive and can serve as dielectric separators. Adjacent graphene sheets can be connected through bonded OFGs via hydrogen bonding. Such bonded GO sheets can be visualized as a sequence of graphene-OFG-graphene

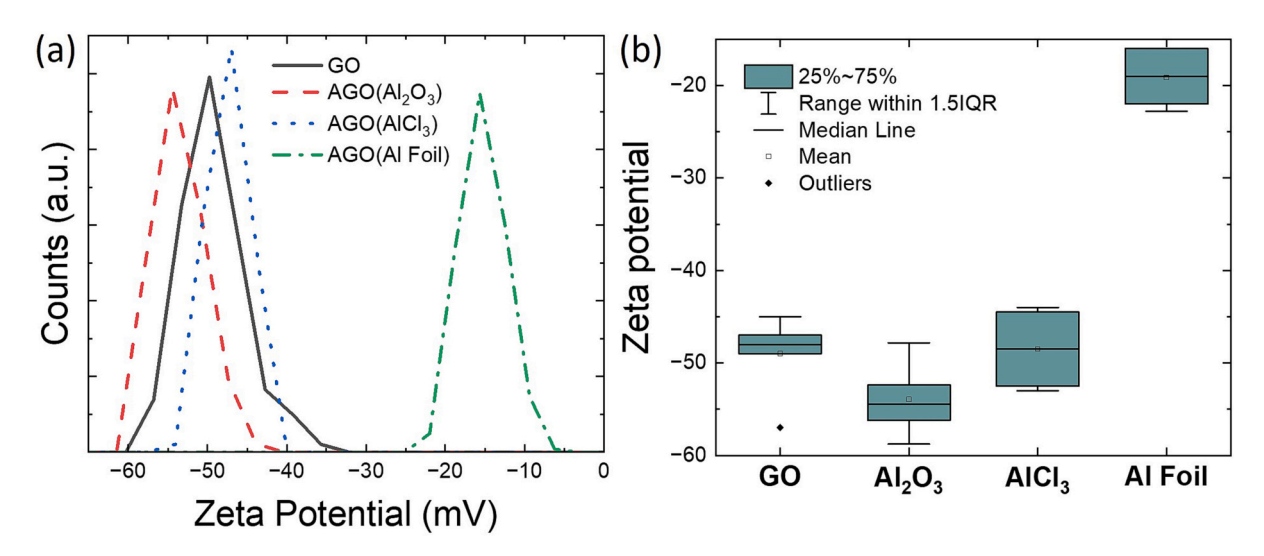


Fig. 2. Zeta potential of GO and AGO dispersions. The zeta potential of AGO (Al foil) is significantly lower in magnitude than the three other membranes. This decreased zeta potential reflects a lower density of negatively charged surface OFGs and an increased propensity for flocculation of the AGO (Al foil) material.

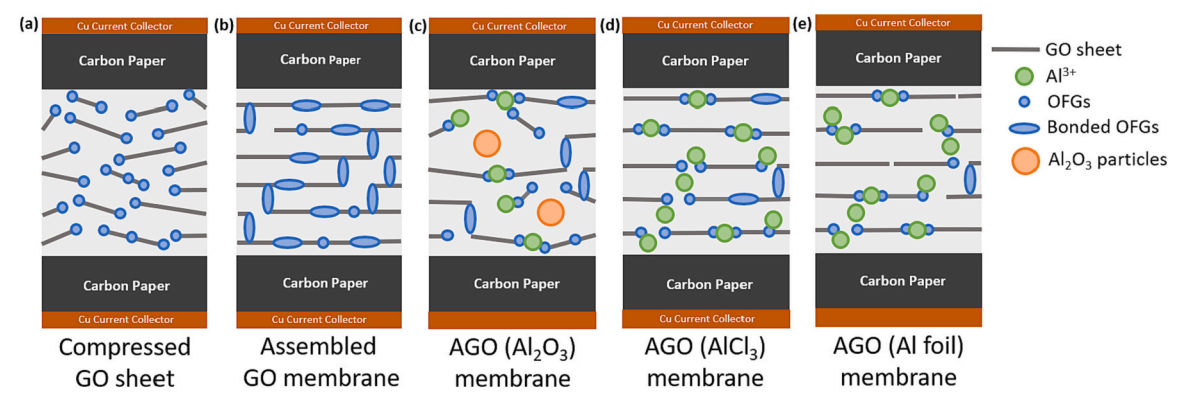


Fig. 3. Schematic representation of carbon paper capacitors with GO/AGO dielectric separators.

2D nanocapacitors connected in series and/or parallel. These membranes exhibit a much lower DiC value than both unbonded (pressed) GO sheet and polymer hybrid GO composites [6-9]. The stacking of GO sheets in both compressed GO sheets and polymer hybrid GO composites (Fig. 3a) are disordered and lack strong inter/intralayer bonding. In contrast, the self-assembled GO membrane (Fig. 3b) is highly ordered by van der Waals interactions between  $\pi$  orbitals and hydrogen bonding interactions between the OFGs of adjacent GO sheets. Those interactions not only connect the adjacent GO sheet, but also guide the GO sheet to form a uniform "brick-and-mortar" stacking configuration, giving rise to the nanochannels in GO membranes through which polar solvents and ions can permeate. Introduction of Al3+ from all three precursors increases the spacing between layers (Fig. 3c, d, e) and Al3+ ions (green) coordinate with the OFGs. Among the three Al3+ sources, Al2O3 releases the fewest free Al<sup>3+</sup> cations through reaction with acidic GO solution; remaining alumina particles disrupt the lamellar structure and decrease the GO membrane stability (Fig. 3c) [19]. This increased disorder results in a higher DiC for AGO(Al<sub>2</sub>O<sub>3</sub>) relative to laminated pristine GO membranes. In contrast to Al<sub>2</sub>O<sub>3</sub>, AlCl<sub>3</sub> (Fig. 3d) and Al foil (Fig. 3e) release significant concentrations of Al<sup>3+</sup> cations when dissolved in the acidic GO solution. Partial reduction of the GO membrane by reaction with Al foil results in fewer OFGs in AGO (Al foil) relative to AGO (AlCl<sub>3</sub>) and AGO (Al<sub>2</sub>O<sub>3</sub>). Since graphene is highly conductive, this partial reduction increases the conductivity of AGO (Al foil) as reflected in the lower dielectric constant (Fig. 1a) and lower capacitance (Fig. 4a) of this membrane. In summary, this microscopic model explains the observed pattern of DiC for these four materials. Increased disorder of the AGO (Al<sub>2</sub>O<sub>3</sub>) membrane (Fig. 3c) increases the DiC, while partial reduction of the AGO(Al foil) membrane (Fig. 3e) decreases the DiC relative to pristine GO at all frequencies. In AGO(AlCl<sub>3</sub>) (Fig. 3c), the greater Al<sup>3+</sup>

complexation with OFGs leads to an increase of DiC specifically at low frequencies due to greater dipole polarization.

As discussed above, our model of the material properties also supports the DiL observations. The low frequency DiL of all AGO membranes is greater than that of GO due to the increased spacing between layers (Fig. 3c, d, e) and accompanying increased energy dissipation by interfacial polarization. The resonance peak in the DiL spectra due to dipole reorientation shifts to lower frequencies for the AGO(AlCl<sub>3</sub>) and AGO (Al foil). Both of these membranes have greater Al<sup>3+</sup>-OFG complexation (Fig. 3d, e), which increases the moment of inertia of the OFGs and thus shifts the resonance frequency to lower values.

Fig. 4a shows cyclic voltammetry (CV) curves for dielectric capacitors using carbon paper electrodes and GO or AGO membrane as the dielectric separator. The scan rate ( $\nu$ ) was set to 100 mV/s with a potential window ( $\Delta$ V) of -1.0 to 1.0 V. The CV curves of all capacitors at different scan rates from 5 to 100 mV/s are summarized in Fig. S2. As the DiC value (at 100 Hz) of the separator material increases, the area of the CV curve increases. The specific capacitance, power, and energy could be estimated using Eqs. (4)–(6).

$$C = \frac{Area \ of \ CV \ curve}{2\nu m\Delta V} \tag{4}$$

$$SP = \frac{Area \ of \ CV \ curve}{...} \tag{5}$$

$$SE = \frac{C\Delta V^2}{2} \tag{6}$$

where  $\nu$  (V/s) is the scan rate, m (kg) is weight combination of carbon paper electrode and GO or AGO dielectric membrane,  $\Delta V(V)$  is the po-

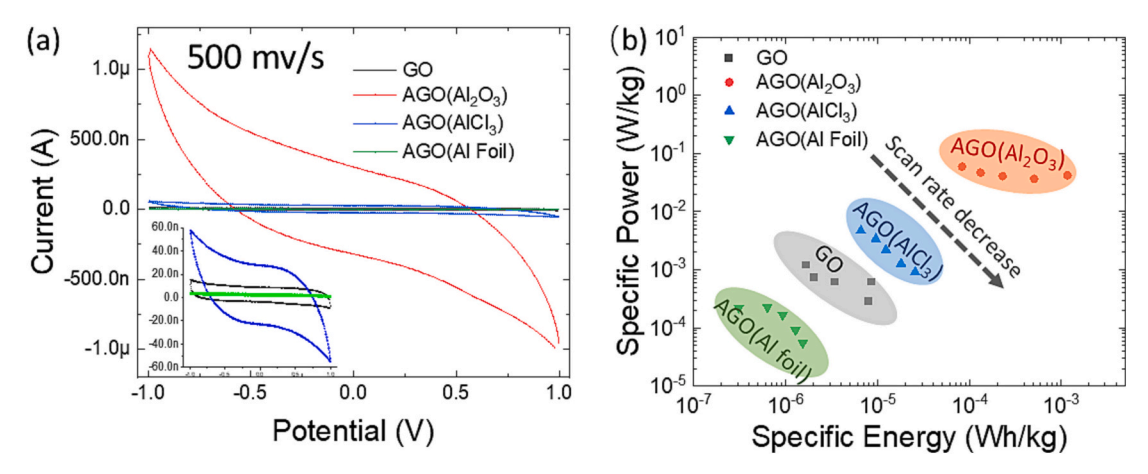


Fig. 4. (a) Cyclic voltammetry (CV) curve and (b) Ragone plot of carbon paper capacitors with GO, AGO (Al $_2$ O $_3$ ), AGO (AlCl $_3$ ), and AGO (Al foil) as dielectric separators in a potential window of  $\pm 1$  V.

tential window, C (F/kg) is specific capacitance, SP (W/kg) is specific power, and SE (Wh/kg) is the specific energy.

According to Eqs. (5) and (6), the specific power and energy of the carbon paper-GO/AGO membrane-carbon paper dielectric capacitor can be summarized in a Ragone plot as shown in Fig. 4b. The absolute C, SP, SE value for such a sandwich structured dielectric capacitor is extremely low due to the carbon paper electrode and current collection copper tape used in the setup. As shown in Fig. 4b, specific power and specific energy increase as the DiC value of the GO/AGO dielectric separator increases from AGO (Al foil) to AGO(Al<sub>2</sub>O<sub>3</sub>). Most strategies for tailoring the functionality of dielectric separator materials have been focused on increasing either the specific power or the specific energy of the capacitor, but the next generation of energy storage and transfer devices will operate in the regime of both higher specific power and energy. In our study, carbon paper capacitors fabricated with a dielectric layer of higher dielectric constant at the operating frequency have both higher specific power and specific energy.

The long-term stability of GO/AGO-based capacitors was studied through 500 charge-discharge cycles with a scan rate of 500 mV/s as shown in Fig. 5. The all-solid-state capacitors with GO, AGO (AlCl<sub>3</sub>) and AGO (Al foil) dielectric separators can retain 100 % capacitance with a 1 % increase per hundred cycles, indicating the excellent stability of GO based capacitors. The capacitor fabricated with AGO (Al<sub>2</sub>O<sub>3</sub>) exhibits a larger capacitance increase of about 3 % per hundred cycles during the cycle stability study range.

### 4. Conclusions

In this work, Al<sup>3+</sup> ions were incorporated into GO membranes by the addition of Al<sub>2</sub>O<sub>3</sub>, AlCl<sub>3</sub>, or Al foil to an acidic GO solution prior to membrane formation. The dielectric performance of GO and AGO membranes were evaluated and explained through inter/intra sheet bonding mechanisms. At the high frequency range of the study, all the GO and AGO membranes show a similar dielectric constant value of 5  $\pm$ 0.5 (1 MHz) and this value increases with decreasing frequency. The addition of Al<sup>3+</sup> through Al<sub>2</sub>O<sub>3</sub> is effective in increasing the dielectric constant, but also increasing the dielectric loss of the GO membrane. Compared to unmodified GO membranes, the addition of Al<sup>3+</sup> through AlCl<sub>3</sub> is effective in increasing the dielectric constant in the low frequency range (1-500 Hz), but decreases the dielectric constant in the higher frequency range (500 Hz  $\sim 1$  MHz). Unlike the other two, the addition of Al<sup>3+</sup> through Al foil decreases the dielectric constant due to partial reduction of the GO sheets. For all AGOs, the dielectric loss peak shifts toward a lower frequency value with cation modification, which likely results from slower dipole reorientation due to greater Al<sup>3+</sup>-OFG complexation. Finally, CV and cycle stability tests were conducted for all GO and AGO membranes when forming an all-solid-state carbon paper capacitor with GO/AGO dielectric separators. The specific capacitance, power, and energy of the capacitors increases in the order AGO(Al foil) < GO < AGO(AlCl<sub>3</sub>) < AGO(Al<sub>2</sub>O<sub>3</sub>), in agreement with the measured dielectric constant at the CV operating frequency (100 Hz). In addition, the as-fabricated solid-state capacitors show excellent cycle stability within the 1000 cycle test. These results demonstrate that the addition of Al3+ from different sources impacts the dielectric properties of the GO membrane and thus the electrochemical performance of the dielectric capacitor using those membranes. The chemical approaches to tailoring dielectric materials shown here will be valuable tools in the development of advanced energy storage devices.

# Novelty statement

This study shows a facile and effective strategy for tailoring the dielectric properties of graphene oxide membranes for potential energy storage devices applications.

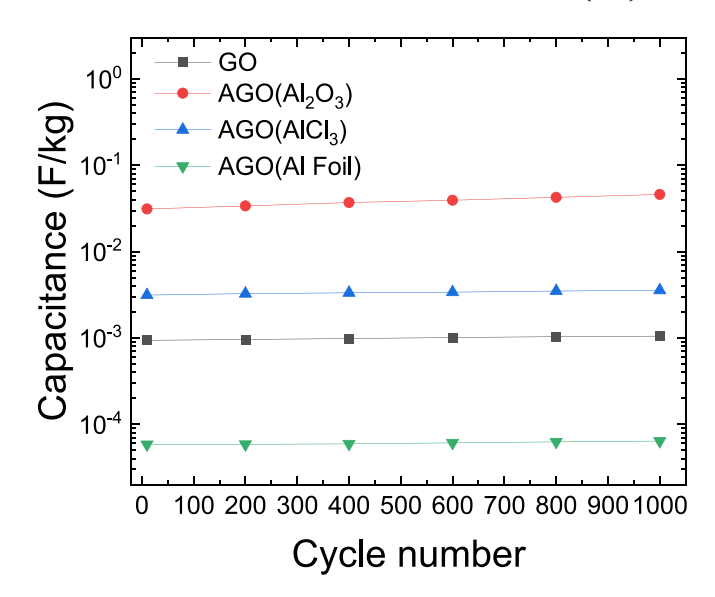


**Fig. 5.** Cycle stability of C-GO-C, C-AGO( $Al_2O_3$ )-C, C-AGO( $AlCl_3$ )-C, and C-AGO(Al foil)-C capacitor with scan rate of 500 mv/s and potential window of +1 V.

# Generative AI in writing statement

During the preparation and revision of this work, authors did not used any generative AI and AI-assisted technologies. Author takes full responsibility for the content of the publication.

### CRediT authorship contribution statement

Y.Y.S: conceptualization, methodology, formal analysis, investigation, visualization, software, writing original draft; M. F.: conceptualization, methodology; T.J.B.: conceptualization, investigation, writing—review and editing; Q. Z. conceptualization—review and editing. All authors gave final approval for publication and agreed to be held accountable for the work performed therein.

# **Declaration of competing interest**

The authors declare that they have no known competing financial interests or personal relationships that could have appeared to influence the work reported in this paper.

# Data availability

The authors declare that the data supporting the findings of this study are available within the paper and supplement.

# Acknowledgements

This work was primarily supported by the National Science Foundation under grant number CMMI 23-01838. M. F. is grateful for Scholar program and Student Research Grant funding from Union College.

# Appendix A. Supplementary data

Supplementary data to this article can be found online at https://doi. org/10.1016/j.diamond.2023.110601.

### References

 C.-N. Yeh, K. Raidongia, J. Shao, Q.-H. Yang, J. Huang, On the origin of the stability of graphene oxide membranes in water, Nat. Chem. 7 (2015) 166–170, https://doi.org/10.1038/nchem.2145.

- [2] D.A. Dikin, S. Stankovich, E.J. Zimney, R.D. Piner, G.H.B. Dommett, G. Evmenenko, S.T. Nguyen, R.S. Ruoff, Preparation and characterization of graphene oxide paper, Nature 448 (2007) 457–460, https://doi.org/10.1038/ nature06016
- [3] B. Mi, Graphene oxide membranes for ionic and molecular sieving, Science 343 (2014) 740–742, https://doi.org/10.1126/science.1250247.
- [4] K.-Y. Chan, A. Baktash, B. Demir, E.L.H. Mayes, D. Yang, D.Q. Pham, K.-T. Lin, A. P. Mouritz, A.S.M. Ang, B. Fox, B. Zhu, H. Lin, B. Jia, K.-T. Lau, Tailoring mechanical and electrical properties of graphene oxide film for structural dielectric capacitors, J. Power Sources 482 (2021), 229020, https://doi.org/10.1016/j.jpowsour.2020.229020.
- [5] S. Al-Zangana, M. Iliut, G. Boran, M. Turner, A. Vijayaraghavan, I. Dierking, Dielectric spectroscopy of isotropic liquids and liquid crystal phases with dispersed graphene oxide, Sci. Rep. 6 (2016) 31885, https://doi.org/10.1038/srep31885.
- [6] K.S. Kumar, S. Pittala, S. Sanyadanam, P. Paik, A new single/few-layered graphene oxide with a high dielectric constant of 10<sup>6</sup>: contribution of defects and functional groups, RSC Adv. 5 (2015) 14768–14779, https://doi.org/10.1039/C4RA10800K.
- [7] A.E.M. Abd Elhamid, H. Shawkey, A.A. Nada, M. Bechelany, Anomalous dielectric constant value of graphene oxide/polyvinyl alcohol thin film, Solid State Sci. 94 (2019) 28–34, https://doi.org/10.1016/j.solidstatesciences.2019.05.013.
- [8] P. Liu, Z. Yao, J. Zhou, Mechanical, thermal and dielectric properties of graphene oxide/polyimide resin composite, High Perform. Polym. 28 (2015) 1033–1042, https://doi.org/10.1177/0954008315613558.
- [9] K. Deshmukh, M.B. Ahamed, K.K. Sadasivuni, D. Ponnamma, R.R. Deshmukh, S.K. K. Pasha, M.A.A. Al Maadeed, K. Chidambaram, Graphene oxide reinforced polyvinyl alcohol/polyethylene glycol blend composites as high-performance dielectric material, J. Polym. Res. 23 (2016) 159, https://doi.org/10.1007/s10965-016-1056-8.
- [10] Z. Wang, R. Wei, X. Liu, Dielectric properties of reduced graphene oxide/copper Phthalocyanine nanocomposites fabricated through π-π interaction, J. Electron. Mater. 46 (2017) 488–496, https://doi.org/10.1007/s11664-016-4916-4.
- [11] W. Gao, N. Singh, L. Song, Z. Liu, A.L.M. Reddy, L. Ci, R. Vajtai, Q. Zhang, B. Wei, P.M. Ajayan, Direct laser writing of micro-supercapacitors on hydrated graphite oxide films, Nat. Nanotech. 6 (2011) 496–500, https://doi.org/10.1038/ pppge 2011.11
- [12] J. Liu, D. Galpaya, M. Notarianni, C. Yan, N. Motta, Graphene-based thin film supercapacitor with graphene oxide as dielectric spacer, Appl. Phys. Lett. 103 (2013), 063108, https://doi.org/10.1063/1.4818337.
- [13] A. Li, K. Han, Y. Zhou, H. Ye, G. Liu, H.H. Kung, Incorporating multivalent metal cations into graphene oxide: towards highly-aqueous-stable free-standing membrane via vacuum filtration with polymeric filters, Mater. Today Commun. 11 (2017) 139–146. https://doi.org/10.1016/j.mtcomm.2017.04.002.

- [14] X.-B. Lv, R. Xie, J.-Y. Ji, Z. Liu, X.-Y. Wen, L.-Y. Liu, J.-Q. Hu, X.-J. Ju, W. Wang, L.-Y. Chu, A novel strategy to fabricate cation-cross-linked graphene oxide membrane with high aqueous stability and high separation performance, ACS Appl. Mater. Interfaces 12 (2020) 56269–56280, https://doi.org/10.1021/acsami.0c15178.
- [15] L. Chen, G. Shi, J. Shen, B. Peng, B. Zhang, Y. Wang, F. Bian, J. Wang, D. Li, Z. Qian, G. Xu, G. Liu, J. Zeng, L. Zhang, Y. Yang, G. Zhou, M. Wu, W. Jin, J. Li, H. Fang, Ion sieving in graphene oxide membranes via cationic control of interlayer spacing, Nature 550 (2017) 380–383, https://doi.org/10.1038/nature24044.
- [16] T. Liu, B. Yang, N. Graham, W. Yu, K. Sun, Trivalent metal cation cross-linked graphene oxide membranes for NOM removal in water treatment, J. Membr. Sci. 542 (2017) 31–40, https://doi.org/10.1016/j.memsci.2017.07.061.
- [17] Y. Long, K. Wang, G. Xiang, K. Song, G. Zhou, X. Wang, Molecular channels directed by cation-decorated graphene oxide nanosheets and their application as membrane reactors, Adv. Mater. 29 (2017) 1–7, https://doi.org/10.1002/ adma.201606093.
- [18] W. Yu, T. Yu, N. Graham, Development of a stable cation modified graphene oxide membrane for water treatment, 2D Mater. 4 (2017), https://doi.org/10.1088/ 2053-1583/aa814c.
- [19] E.J. Robertson, Y.Y. Stehle, X. Hu, L. Kilby, K. Olsson, M. Nguyen, R. Cortez, Al<sup>3+</sup> modification of graphene oxide membranes: effect of Al source, Membranes 12 (2022) 1237, https://doi.org/10.3390/membranes12121237.
- [20] Y.Y. Stehle, E.J. Robertson, R. Cortez, R.B. Bucinell, I.V. Vlassiouk, In-plane and through-plane dielectric properties of graphene oxide membrane: effect of Al<sup>3+</sup> modification, Materialia 23 (2022), 101442, https://doi.org/10.1016/j. mtla.2022.101442.
- [21] A. Schönhals, F. Kremer, Analysis of dielectric spectra, in: F. Kremer, A. Schönhals (Eds.), Broadband Dielectric Spectroscopy, Springer, Berlin, 2003, pp. 59–98.
- [22] P. Kumar, S. Penta, S.P. Mahapatra, Dielectric properties of graphene oxide synthesized by modified Hummers' method from graphite powder, Integr. Ferroelectr. 202 (2019) 41–51, https://doi.org/10.1080/ 10584587.2019.1674822.
- [23] B. Konkena, S. Vasudevan, Understanding aqueous dispersibility of graphene oxide and reduced graphene oxide through pK<sub>a</sub> measurements, J. Phys. Chem. Lett. 3 (2012) 867–872, https://doi.org/10.1021/jz300236w.
- [24] X. Hu, Y. Yu, W. Hou, J. Zhou, L. Song, Effects of particle size and pH value on the hydrophilicity of graphene oxide, Appl. Surf. Sci. 273 (2013) 118–121, https://doi. org/10.1016/j.apsusc.2013.01.201.
- [25] K. Krishnamoorthy, M. Veerapandian, K. Yun, S.-J. Kim, The chemical and structural analysis of graphene oxide with different degrees of oxidation, Carbon 53 (2013) 38–49. https://doi.org/10.1016/j.carbon.2012.10.013.